

Influence of Ta-based Diffusion Barriers on the Microstructure of Copper Thin Films

M. STANGL,^{1,4} A. FLETCHER,² J. ACKER,^{1,3} H. WENDROCK,¹ and K. WETZIG¹

1.—IFW Dresden, P.O. Box 27 01 16, 01171 Dresden, Germany. 2.—University of British Columbia, Vancouver, BC, Canada V6T 1Z1. 3.—University of Applied Sciences Lausitz, P.O. Box 10 15 48, 01958 Senftenberg, Germany. 4.—e-mail: M.Stangl@ifw-dresden.de

Copper represents the most commonly used interconnect material in ultra large-scale integration (ULSI) technology. Given that the successful implementation of Cu requires the use of underlying diffusion barriers, these studies were focused on the influence of Ta-based barrier layers on the microstructure of physical vapor deposited (PVD) and electrochemically deposited (ECD) Cu thin films. The variation of α -Ta, β -Ta, TaSiN, and TaN as an underlayer caused a modification of the PVD Cu seed-layer texture, which also affected the microstructure of Cu electroplated on top of the seed layer, both before and after recrystallization at room temperature.

Key words: Barrier, copper, electrochemical deposition, microstructure, self-annealing

INTRODUCTION

Copper has become the material of choice for interconnects in semiconductor devices due to its low resistivity and high resistance against electromigration.¹ The deposition of Cu is commonly performed by electroplating and shows an excellent filling of trenches with high aspect ratio. According to earlier studies,^{2–4} freshly electroplated films exhibit a crystal transition with increasing layer thickness from a basis-oriented texture reproduction type (BR) into a field-oriented texture type (FT). The BR crystals reproduce the texture of the underlying substrate, whereas the FT structure is influenced by plating conditions such as applied current density, additive content, and temperature. For manufacturing of Cu interconnects, the underlying substrate consists of a thin PVD Cu seed-layer deposited on a Cu diffusion barrier, as shown schematically in Fig. 1.

Recent publications indicate that the texture of PVD Cu exhibits crystallographic differences depending on the underlying substrate.^{5–10} Hence,

different barrier systems should also lead to changes of both initial PVD and ECD Cu texture. The present paper will discuss the effect of various barrier layers on the initial microstructure of PVD and freshly electroplated Cu thin films. Furthermore, it will be revealed how the Cu recrystallization process at room temperature (self-annealing¹¹) changes with variation of barrier material. These studies are limited to α -Ta, β -Ta, TaSiN, and TaN as most diffusion barriers consist of Ta-based metallizations.

EXPERIMENTAL

The electrochemical deposition of Cu was carried out with a FIBRoplateTM IKOTM plating station (ECSI FIBRtools Company, Denville, NJ, USA). The electrolyte solution contained a typical composition^{12–15} of 0.25 M CuSO₄ · 5H₂O, 1.8 M H₂SO₄, and 1.41 mM Cl⁻ in the form of KCl (all chemicals p.A., Merck, Germany). Two commercially available additives, SC MD and SC LO 70/30 (Enthone Inc., Germany), were added to obtain smooth and defect-free blanket Cu films. A DC current density of 15 mA/cm² was applied to generate Cu layers up to 2,000 nm in thickness. As substrate material,

(Received May 31, 2007; accepted August 20, 2007; published online September 19, 2007)

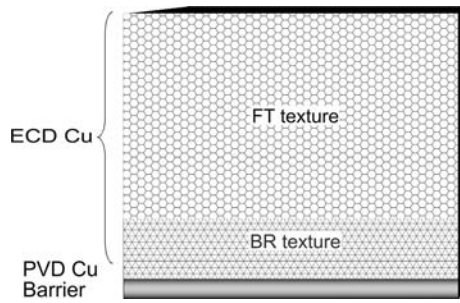


Fig. 1. Schematic build-up indicating the initial texture of an ECD Cu film deposited on a PVD Cu seed layer with underlying diffusion barrier.

thermally oxidized Si(100) blanket wafers were chosen. Using magnetron sputtering without a vacuum break, we deposited a 50 nm diffusion barrier and a 50 nm PVD Cu seed layer. The barrier impedes Cu diffusion into the SiO₂ and acts as an adhesion promoter between the Cu layer and substrate by chemical bonding.¹⁶ Ta, TaSiN, and TaN films were radio-frequency magnetron sputtered. Tetragonal β -Ta is formed directly by deposition on SiO₂ whereas the body centered cubic α -Ta is induced by an underlying 30 nm TaN layer.¹⁷

The investigation of initial texture and self-annealed microstructure was done by electron backscatter diffraction (EBSD). An analysis software from HKL Technology was used to extract texture information. The maximum information depth of EBSD in Cu is roughly 60 nm.¹⁸ For the determination of (111) texture fraction from EBSD measurements, the area fraction of the (111) component parallel to the sample normal (Z plane) with a maximum misorientation angle of 7° was considered. Small EBSD mappings with a 100 × 100 raster and 0.05 μ m step size were used for initial texture investigations. Recrystallized Cu thin films were analyzed by large EBSD mappings up to 10⁵ μ m² area using a step size of 0.25 μ m.

The resistivity changes in consequence of microstructure evolution could be monitored by an in-house fabricated four-point probe resistivity measuring system. Here it is well established that the resistivity decreases during grain growth as a result of a shrinking amount of electron scattering at grain boundaries in accordance with the Mayadas-Shatzkes model.^{19,20} A laser-optical wafer-curvature measurement system (Flexus, Tencor Instruments) was applied for investigation of stress relaxation during self-annealing. X-ray diffraction (XRD) was performed using a Philips X'pert device. Focused ion beam (FIB) investigations were carried out with a FIB Crossbeam 1540 XB (Zeiss).

RESULTS AND DISCUSSION

It was found, that the electrochemical deposition of Cu is not homogeneous with increasing film thickness with respect to the crystal orientation.

Table I. Decreasing (111) Texture Fraction for Increasing Film Thickness of PVD Cu Layers

PVD Cu film thickness (nm)	50	600	1000
Initial (111) texture fraction (%)	97	32	16

The first formed ECD Cu crystals reproduce the texture of the underlying PVD Cu followed by a rapid transition into a FT texture type. In correlation with electroplating, the PVD sputter process generates Cu layers revealing a change in texture with increasing film thickness. Table I indicates that this texture transition is not as rapid as for ECD Cu layers, which is confirmed by other studies.^{5,21} Remarkably, the 1,000 nm PVD Cu layer showed a slow microstructure evolution and about 15% of the fine-grained microstructure were recrystallized within 1.5 years after deposition. This grain growth is assumed to originate from an induced self-annealing process analogous to electroplated Cu thin films.

The texture of PVD Cu is influenced by different diffusion barrier systems.^{5–10} EBSD measurements obtained a strong (111) fiber texture (97% (111) fraction) for a 50 nm Cu seed-layer deposited on a 50 nm Ta barrier. This tetragonal β -Ta changes into b.c.c. α -Ta if it is grown on a TaN film.¹⁷ However, the PVD Cu microstructure was found to be similar for α -Ta and β -Ta-based metallizations. The application of 50 nm TaSiN and 50 nm TaN, respectively, led to less strong (111) oriented PVD Cu layers. For PVD Cu on TaSiN the (111) fraction was 50% and in the case of TaN 19% of (111) fraction were obtained. XRD measurements confirmed these results by comparing the normalized (111) pole plots of 50 nm PVD Cu films sputtered on β -Ta, TaSiN, and TaN, as shown in Fig. 2. With decreasing (111) texture (511) twins and other randomly oriented crystals arise. FIB top view images (Fig. 3) also revealed these qualitative differences in crystal texture through the strong orientation contrast in ion-induced secondary electron images.

Lee et al.⁷ revealed the interface bonding strength between Cu and the underlying barrier as an important factor of influence leading to differences in the Cu crystal orientation. This correlates with the theory of heterogeneous nucleation of solid films on planar substrates,²² where the film growth strongly depends on the surface properties of the involved materials. The similar microstructure of PVD Cu deposited on α -Ta and β -Ta confirms this result as the characteristic Cu/Ta interface energy remains almost unchanged. Since a strong Cu (111) texture is ascribed to a better interface-wetting, the Cu/barrier interface bonding strength should differ such that Ta > TaSiN > TaN. Theoretical calculations support this assumption by determining a 20% higher surface chemical affinity for the Cu/Ta system compared with the Cu/TaN system.²³

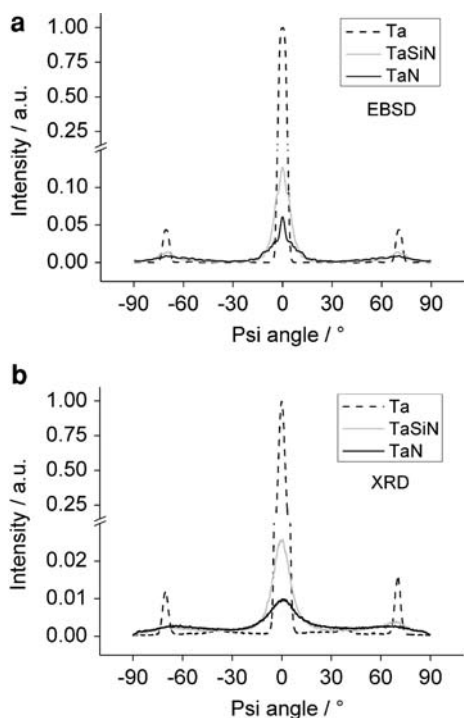


Fig. 2. Normalized (111) pole plots determined from (a) EBSD and (b) XRD measurements on 50 nm PVD Cu films deposited on β -Ta, TaSiN, and TaN.

Furthermore, since Si exhibits a 2/3 lower surface energy than Ta, we speculate that this could be an indicator for the medium interface bonding strength of the Cu/TaSiN system.²⁴

If an ECD Cu film is deposited on the Cu seed-film, the BR crystals change more rapidly into the FT structure in the case of a less strong (111) oriented substrate. Figure 4 illustrates corresponding EBSD results for electroplated Cu layers on 50 nm PVD Cu and 50 nm diffusion barrier consisting of β -Ta, TaSiN, and TaN. As the exchange current density is known to be dependent on the crystal

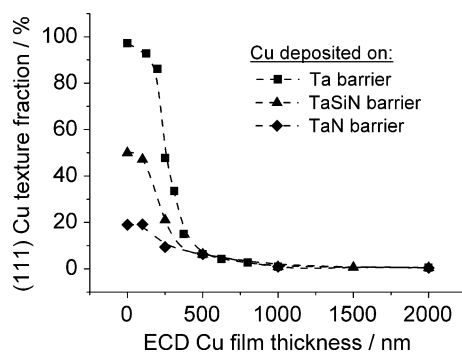


Fig. 4. (111) texture fraction versus film thickness obtained by EBSD for Cu films electroplated on 50 nm PVD Cu seed layer and 50 nm diffusion barrier consisting of β -Ta, TaSiN, or TaN, measured in the as-deposited state.

orientation, the resulting differences in crystal growth rates could represent a crucial factor for the faster transition into the field-oriented texture type.²⁵

The recrystallization of electroplated Cu is also influenced by different diffusion barrier systems, where here the substrate material affects the texture of freshly deposited Cu films.^{26,27} In general, the higher the volume fraction of (111) oriented crystals, the slower the kinetics of self-annealing proceeds due to the dominance of low angle grain boundaries exhibiting a low energy and mobility.²⁸ The resistivity and stress curves for 2,000 nm electroplated Cu layers support this theory for the accelerated recrystallization process in the order of TaN > TaSiN > β -Ta-based metallizations (Fig. 5). In the case of TaN system, the recrystallization of Cu is finished within 2.5 h, whereas a TaSiN-based system needs 6 h and a β -Ta-based system revealed 15 h for Cu self-annealing. Resistivity and compressive stress decreases during this time. The maximum values of initial compressive stress appear in the order TaN > TaSiN > β -Ta indicating

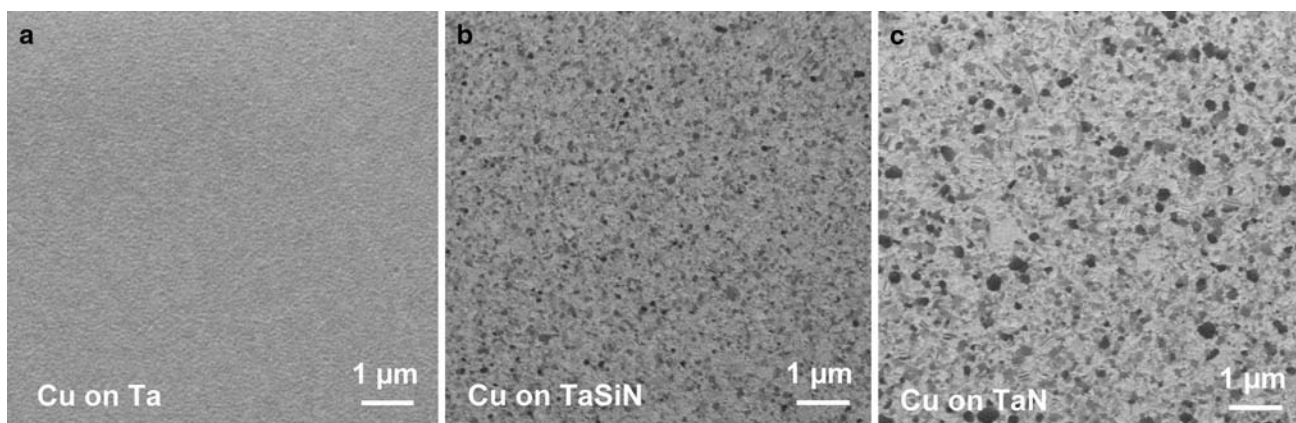


Fig. 3. FIB top view images of 50 nm PVD Cu films deposited on β -Ta, TaSiN, and TaN.

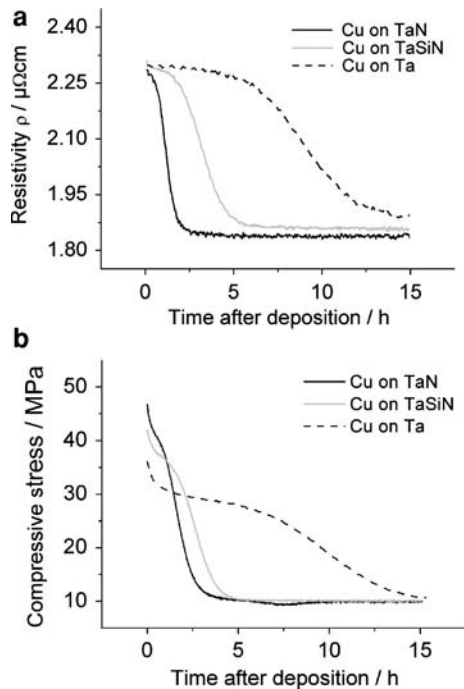


Fig. 5. Resistivity and stress curves of 2,000 nm ECD Cu films deposited on 50 nm β -Ta, TaSiN, and TaN diffusion barriers.

compressive stress as an important driving force for thin film recrystallization.

The end of self-annealing is characterized by an almost stress-free state and a stabilized coarse-grained microstructure. As shown in Table II, an accelerated Cu self-annealing leads to a decreased mean grain size after recrystallization. According to the theory of nucleation and crystal growth, a faster grain growth requires more nuclei growing at the same time leading to a more small-grained microstructure.^{29,30} Inverse pole figures obtained by

EBSD for self-annealed Cu films revealed a preferred (111) orientation. The strength of the (111) texture is comparable for β -Ta and TaN-based metallizations but is three times stronger for the TaSiN-based system. The (511) component, representing the first generation annealing twins of (111) oriented crystals, increases in strength for a stronger (111) fiber texture. In the case of a Ta-based metallization the recrystallized microstructure exhibits a (331) component in addition to the (111) and (511) texture.

CONCLUSIONS

EBSD texture analyses and investigations of Cu self-annealing were carried out for PVD and ECD Cu films deposited on Ta-based diffusion barriers. The obtained results indicate the following.

- Ta-based diffusion barriers influence the texture of PVD and ECD Cu thin films.
- The Cu/barrier interface bonding energy is assumed as an important determining factor for differences in Cu texture.
- With increasing Cu layer thickness, the texture changes from a basis reproduction type into a field-oriented type.
- Differences in the volume fraction of (111) Cu crystals lead to changes in the kinetics of Cu self-annealing.
- Less strong (111) textured Cu thin films exhibit an accelerated recrystallization.
- After microstructure evolution, the smallest mean grain size was obtained for Cu films showing the fastest self-annealing due to the theory of nucleation and crystal growth.

In conclusion, it was found that for Cu interconnects the Cu/Ta system exhibits the best properties. The large mean grain size after recrystallization is significant for the enhancement of electromigration

Table II. Time for Self-annealing, Final Grain Size and EBSD Inverse Pole Figures of 2 μm Cu Thin Films Deposited on β -Ta, TaSiN, and TaN Diffusion Barriers

Diffusion Barrier	β -Ta	TaSiN	TaN
Time for ECD Cu self-annealing/h	15	6	2.5
Cu grain size after self-annealing/ μm	5.1	3.9	3.4
EBSID inverse pole figure (Z plane) of 2 μm ECD Cu films after self-annealing			

resistance.³¹ Furthermore, the strong Cu/Ta interface bonding in comparison to TaN and TaSiN-based metallizations represents an enormous advantage.

ACKNOWLEDGEMENTS

The authors would like to thank DAAD, UBC, and DFG for the financial support. Furthermore, the manufacturing of diffusion barriers (Ta, TaSiN, TaN) and Cu seed layer on Si(100) samples by R. Kaltofen is gratefully acknowledged.

REFERENCES

1. S.P. Murarka, I.V. Verner, and R.J. Gutmann, *Copper – Fundamental Mechanisms for Microelectronic Applications* (Wiley, 2000).
2. G.I. Finch, *Z. Elektrochemie* 56(6), 457 (1950).
3. H. Fischer, *Elektrolytische Abscheidung und Elektrokrystallisation von Metallen* (Springer, 1954).
4. N.A. Pangarov, *J. Electroanal. Chem.* 9, 70 (1965).
5. D.P. Field, J.E. Sanchez, N.J. Park, and P.R. Besser, *Mat. Sci. Forum* 495–497, 1323 (2005).
6. D.D. Fong (Ph.D. dissertation, Harvard University, 2001).
7. H. Lee and S.D. Lopatin, *Thin Solid Films* 492(1–2), 279 (2005).
8. R.P. Vinci (Ph.D. dissertation, Stanford University, 1994).
9. E. Zschech, W. Blum, I. Zienert, and P.R. Besser, *Z. Metallkunde* 92(7), 803 (2001).
10. W.M. Kuschke, A. Kretschmann, R.M. Keller, R.P. Vinci, C. Kaufmann, and E. Arzt, *J. Mater. Res.* 13(10), 2962 (1998).
11. M. Stangl, J. Acker, V. Dittel, W. Gruner, V. Hoffmann, and K. Wetzig, *Microelectr. Eng.* 82(2), 182 (2005).
12. C. Gabrielli, P. Mocoteguy, H. Perrot, D. Nieto-Sanz, and A. Zdunek, *Electrochim. Acta* 51(8–9), 1462 (2006).
13. M. Militzer, P. Freundlich, and D. Bizzotto, *Mat. Sci. Forum* 467–470, 1339 (2004).
14. S. Miura and H. Honma, *Surf. Coat. Technol.* 169–170, 91 (2003).
15. T.P. Moffat, D. Wheeler, and D. Jossell, *J. Electrochem. Soc.* 151(4), C262 (2004).
16. S.P. Murarka, *Mater. Sci. Eng. R* 19(3–4), 87 (1997).
17. M. Traving, I. Zienert, E. Zschech, G. Schindler, W. Steinhögl, and M. Engelhardt, *Appl. Surf. Sci.* 252(1), 11 (2005).
18. H. Wendrock, S. Menzel, D. Rauser, and K. Wetzig, *Microsc. Microanal.* 9, 128 (2003).
19. J.M.E. Harper, C. Cabral, P.C. Andricacos, L. Gignac, I.C. Noyan, and K.P. Rodbell, *J. Appl. Phys.* 86(5), 2516 (1999).
20. A.F. Mayadas and M. Shatzkes, *Phys. Rev. B* 1(4), 1382 (1970).
21. N.J. Park and D.P. Field, *Scr. Mater.* 54(6), 999 (2006).
22. M. Ohring, *The Materials Science of Thin Films* (San Diego, CA: Academic Press Inc., 1992).
23. H. Simka, S. Shankar, C. Duran, and M. Haverty, *Mater. Res. Soc. Symp. Proc.* 863, 283 (2005).
24. L.Z. Mezey and J. Giber, *Japan J. Appl. Phys.* 21(11), 1569 (1982).
25. P.W. Atkins and J. De Paula, *Physical Chemistry* (Oxford University Press, 2006).
26. K. Pantleon and M.A.J. Somers, *J. Appl. Phys.* 100(11) (2006).
27. E.M. Zielinski, R.P. Vinci, and J.C. Bravman, *J. Appl. Phys.* 76(8), 4516 (1994).
28. F.J. Humphreys and M. Hatherly, *Recrystallization and Related Annealing Phenomena* (Elsevier Science Ltd., 1996).
29. H.J. Bargel and G. Schulze, *Werkstoffkunde* (Springer, 2000).
30. G.E.R. Schulze, *Metallphysik* (Akademie-Verlag, 1974).
31. C.S. Hau-Riege, *Microelectr. Rel.* 44, 195 (2004).